

Predicted cancer risks induced by computed tomography examinations during childhood, by a quantitative risk assessment approach

Neige Journy · Sophie Ancelet · Jean-Luc Rehel ·
Myriam Mezzarobba · Bernard Aubert ·
Dominique Laurier · Marie-Odile Bernier

Received: 23 May 2013 / Accepted: 8 September 2013 / Published online: 9 October 2013
© Springer-Verlag Berlin Heidelberg 2013

Abstract The potential adverse effects associated with exposure to ionizing radiation from computed tomography (CT) in pediatrics must be characterized in relation to their expected clinical benefits. Additional epidemiological data are, however, still awaited for providing a lifelong overview of potential cancer risks. This paper gives predictions of potential lifetime risks of cancer incidence that would be induced by CT examinations during childhood in French routine practices in pediatrics. Organ doses were estimated from standard radiological protocols in 15 hospitals. Excess risks of leukemia, brain/central nervous system, breast and thyroid cancers were predicted from dose–response models estimated in the Japanese atomic bomb survivors’ dataset and studies of medical exposures. Uncertainty in predictions was quantified using Monte Carlo simulations. This approach predicts that 100,000 skull/brain scans in 5-year-old children would result in eight (90 % uncertainty interval (UI) 1–55) brain/CNS cancers and four (90 % UI 1–14) cases of leukemia and that 100,000 chest scans would lead to 31 (90 % UI 9–101) thyroid cancers, 55 (90 % UI 20–158) breast cancers, and one (90 % UI <0.1–4) leukemia case (all in excess of risks

without exposure). Compared to background risks, radiation-induced risks would be low for individuals throughout life, but relative risks would be highest in the first decades of life. Heterogeneity in the radiological protocols across the hospitals implies that 5–10 % of CT examinations would be related to risks 1.4–3.6 times higher than those for the median doses. Overall excess relative risks in exposed populations would be 1–10 % depending on the site of cancer and the duration of follow-up. The results emphasize the potential risks of cancer specifically from standard CT examinations in pediatrics and underline the necessity of optimization of radiological protocols.

Keywords Ionizing radiation · Low doses · Computed tomography · Pediatric · Cancer · Quantitative risk assessment · Uncertainty analysis

Introduction

Computed tomography (CT), which provides substantial medical benefits, is in widespread use in health care (UNSCEAR 2008); for example, 62 million CT scans were performed in the USA in 2006 (Mettler et al. 2008b) and 7.6 million in France in 2007 (Etard et al. 2012). Effective doses of ionizing radiation (IR) from CT scans may be at least 5–20 times higher than those from routine conventional radiology (Shrimpton et al. 1991; Mettler et al. 2008a). Consequently, CT contributes a large portion of overall medical exposure—estimated at 20–70 % depending on country (Mettler et al. 2008b; UNSCEAR 2008; Smith-Bindman et al. 2012). This magnitude of exposure raises concerns about its potential adverse effects, particularly the risks of leukemia and some solid cancers that can be induced by exposure to IR (IARC 2012). These

Electronic supplementary material The online version of this article (doi:10.1007/s00411-013-0491-8) contains supplementary material, which is available to authorized users.

N. Journy · S. Ancelet · M. Mezzarobba · D. Laurier ·
M.-O. Bernier (✉)

Laboratory of Epidemiology, Institut de Radioprotection et de
Sûreté Nucléaire, Fontenay-aux-Roses, France
e-mail: marie-odile.bernier@irsn.fr

J.-L. Rehel · B. Aubert
Medical Radiation Protection Expertise Unit, Institut de
Radioprotection et de Sûreté Nucléaire, Fontenay-aux-Roses,
France

concerns are stronger for pediatric exposure, because children are more sensitive to radiation than adults and because their longer life expectancy is likely to increase lifetime risks. Children are also more likely to undergo repeated CT scans throughout their lifetime. Moreover, some authors have suggested that the doses may be higher in children than in adults because of the failure to optimize radiological parameters relative to body size (Huda and Vance 2007).

Fractionated exposure to X-rays for close medical surveillance by repetitive fluoroscopy or radiography has been related to an increase in cancer risk after high cumulative doses (Boice et al. 1991; Howe and McLaughlin 1996; Ronckers et al. 2008) as radiotherapy for malignant (Sigurdson et al. 2005; Neglia et al. 2006; Tukenova et al. 2011) and benign conditions (Mattsson et al. 1993; Karlsson et al. 1998; Adams et al. 2010) have been. These results support the existence of a significant dose–response relation between X-ray exposure from medical procedures and the risks of cancer of the breast, central nervous system (CNS), and thyroid gland, a relation that is strongest after exposure during childhood. An extensive literature describes strong associations between IR exposure and leukemia (Wakeford 2013). Nonetheless, these results, including those related to medical monitoring, have mostly been associated with cumulative organ doses [of about 0.1 to units or tens of grays (Gy)] that largely exceed the dose range of CT exposures (Ron 2003; Pettorini et al. 2008). Epidemiological studies of diagnostic radiological examinations at usually low doses (<1 to tens of mGy to organs) have so far provided inconsistent results, and they have often been limited by inaccurate dose reconstruction (Schulze-Rath et al. 2008; Linet et al. 2009; Baysson et al. 2012).

The life span study (LSS) of survivors of the atomic bombings of Hiroshima and Nagasaki has provided useful information to help assess radiation-induced risks after acute external exposures (Preston et al. 2007; Richardson et al. 2009; Ozasa et al. 2012; Hsu et al. 2013), from a wide dose range mostly lower than those in the afore mentioned studies of medical high-dose exposure. Up to now, results from the LSS have been the principal source for recommendations for radiation protection. The dose levels from which excess risks have been estimated in this Japanese population (about 100 mGy on average) might still be substantially higher than usual exposures of units to tens of mGy from a single CT. Nevertheless, risk prediction from the LSS suggests that the potential risks of cancer from CT scans may be low for individuals in relation to the expected clinical benefits. It suggests, however, that their collective impact may be substantial, in view of the magnitude of population exposure. Some authors have estimated that in 14 countries with high levels of health care, 0.6–3.2 % of all incident cancers may be attributable to collective

exposure to diagnostic X-rays (Berrington de Gonzalez and Darby 2004) and 1.5–2.0 % of US cancer deaths may be attributable to overall CT exposure there (Brenner and Hall 2007).

Accordingly, large cohort studies have been published (Pearce et al. 2012; Mathews et al. 2013) or are underway to assess the risk of cancer related specifically to CT examinations of children and young adults (Bernier et al. 2012b; Krille et al. 2012). The first analyses have showed excess risks of several cancer types such as brain/CNS tumors and leukemia (Pearce et al. 2012; Mathews et al. 2013). However, dealing with the suggested radiation-induced risks in clinical practice requires a more complete understanding of these results over an extended life period, at other sites where cancer may occur after long latency periods and including the investigation into potential confounders such as underlying clinical conditions.

While awaiting these results, a quantitative risk assessment (QRA) approach would enable the prediction of the lifetime cancer risks that CT scans may induce according to characteristics such as the patient's age and the anatomical area explored. From the standard assumption of a no-threshold dose–response relation (NRC 2006) that may not be modified by fractionated exposures (Preston et al. 2002; Little 2001, 2008), risk estimates derived from the LSS dataset and/or medical high-dose studies could be extrapolated to the context of lower doses received from CT scans, providing that the populations and exposures are comparable in other respects (such as genetic and lifestyle factors potentially involved in radiation-related risks, dose rate, etc).

Accordingly, the magnitude of potential lifetime risks of incidence of leukemia and thyroid, breast (in women only), and brain/CNS cancers, which might be induced by childhood CT examinations in France, are predicted here, using a QRA approach (NCRP 2012). The study is based on the standard radiological protocols used in recent routine practices in pediatrics. The localized exposures over patients' bodies required that specific cancer sites were considered rather than an overall measure of cancer risk and relevant organ doses. We focused on the four cancer sites specified because evidence already shows the radiation sensitivity of the associated tissues and because these organs or tissues are frequently exposed to X-rays in children undergoing CT scans. Here, brain/CNS cancers were defined as malignant and benign tumors and leukemia included all histological types.

Materials and methods

Potentially radiation-induced risks of cancer are predicted for children currently undergoing CT scans in France (the target population), based on selected cancer-specific dose–

response models fitted to the Japanese atomic bomb survivors' dataset and on studies of medical exposures. Predicted lifetime excess risks are given, first, per CT scan according to characteristics at examination, so that risks could be added for a child having repeated examinations. Second, predicting the number of cases that would occur in populations exposed to repeated CT scans during childhood allowed the calculation of the overall relative risks that would be observable. Risk predictions are associated with uncertainty intervals (UI) that reflect the dose variability between the hospitals and over the survey period, as well as uncertainties about the parameters of the dose–response models, the assumption of linear dose–response relation for solid cancers, and the method for population-to-population risk transport.

Data about the target population

Exposure in the target population was characterized based on the French *Enfant Scanner* cohort, which is studying the relation between childhood CT and cancer risk in France (Bernier et al. 2012b). CT scans received by children younger than 10 years from 2004 to 2009 in 15 French university hospitals, that examined any of the following anatomical areas: skull/brain, middle ear, cervical spine, chest, and abdomen + pelvis, were considered here, regardless of the child's clinical condition. During this period, the radiology departments used eight single- and 21 multi-detector CT machines. Organ doses were estimated based on the standard radiological protocols drawn up by each department to define the default technical parameters that could be implemented on the available CT equipment for routine examinations according to the patient's age (or body weight). Radiological protocols (specific to anatomical area, patient's age, CT equipment, use period, and department) were collected in all the hospitals, except for cervical spine and middle ear CTs for which data were available in only seven and 13 hospitals, respectively. We used the numerical simulation software CT-expo (Stamm and Nagel 2002) to generate volume CT dose index ($CTDI_{vol}$) values and estimate organ doses for two phantoms, one the size of 7-week-olds and another of 7-year-olds, assigned to represent the two age groups of interest: <1 and 1–10 years. For each type of CT (defined by the explored anatomical area) and age group, empirical organ dose distributions were characterized by the set of dose values, previously calculated for each radiological protocol, by use period, and hospital, for all examinations over the survey period (only one CT equipment was in use in each department at any given time, except in one hospital for which the mean dose values were considered here because it was unknown which CT machine of the two available was used for each examination).

Cancer-free survival and background risks in the unexposed target population were estimated from cancer incidence and mortality rates in the French general population insofar as CT exposure in childhood was infrequent (Etard et al. 2012). We considered the age- and gender-specific rates in the most recent years, i.e., over the 2000–2005 period, estimated from the French regional cancer registries (Belot et al. 2008) (data were available online http://www.invs.sante.fr/surveillance/cancers/estimations_cancers/default.htm, accessed July 4, 2012) and recorded by the national center for cause-of-death statistics and epidemiology (<http://www.cepidc.vesinet.inserm.fr/>, accessed July 4, 2012). The cancer incidence and mortality rates were assumed to be homogeneously distributed when extrapolating lifetime risks from the period 2000–2005 to the period 2004–2009. Note, however, that leukemia incidence rates included only new diagnoses of acute (all histology codes) and chronic lymphoid leukemia.

Age-specific sex ratios in the general population from 2000 to 2005, estimated from the national census (<http://www.ecosante.fr/index2.php?base=FRAN&langh=FRA&langs=FRA&sessionid>, accessed July 4, 2012), were used for further gender-averaged calculations and were assumed to be constant over the study period.

Dose–response models and excess risk estimation

Dose–response models, based on Poisson's disease models (Breslow and Day 1987), which were estimated from both the LSS and medically exposed populations, were considered pertinent for risk prediction in our target population. The excess absolute risk (EAR) and the excess relative risk (ERR) models proposed by Preston et al. (2002) and Ron et al. (1995), both previously validated in medical studies and in the LSS dataset, were used for prediction of breast and thyroid cancers risks, respectively. For the other sites of cancer, no such meta-analyses have been published to the best of our knowledge. Thus, both additive and multiplicative risk transfer was considered, and the dose–response models proposed by Preston et al. (2007) and the United Nations Scientific Committee on the Effects of Atomic Radiation (UNSCEAR 2006) for describing brain/CNS cancer incidence and leukemia mortality risks, respectively, from the LSS, were considered here.

Table 1 details the dose–response models and the estimated parameters. For breast cancer, the risk coefficient estimates and associated 95 % confidence intervals (CI), published in Preston et al. (2002), were applied directly. For thyroid cancer, risk estimates specific to gender and age at exposure were derived following the approach of the National Research Council (NRC 2006) in the absence of available data. First, an estimate of the unknown coefficient determining the adjustment to the ERR for age

at exposure (considered here as a continuous covariate) was derived, by linearly interpolating the gender-averaged log(ERR) values previously estimated by the US National Institutes of Health (NIH 2003) for age at exposure in increments of 5 years (from Ron et al. (1995)). Next, the probability of a higher radiation-induced effect in females, as emphasized in the primary analysis (Ron et al. 1995) and in a recent report about thyroid cancer incidence in the LSS (Furukawa et al. 2013), was considered. A gender-specific risk coefficient estimate was thus derived by weighting the gender-averaged one by the odds ratio (OR) between genders estimated by Ron et al. (1995) while assuming that the gender and age at exposure effects were independent.

Finally, for leukemia and brain/CNS cancer, the risk coefficients and associated 95 % CIs were estimated by fitting the selected dose–response models to the LSS dataset, available online from the Radiation Effects Research Foundation (RERF) Web site (http://www.rerf.or.jp/library/dl_e/index.html, accessed July 4, 2012) and using Epicure/AMFIT software (Preston et al. 1993). We used both the original dataset of brain/CNS cancer incidence (Preston et al. 2007) and the latest update of leukemia mortality (Ozasa et al. 2012). The dose–response relation between exposure and risk of leukemia incidence was assumed to be relevantly described by mortality data. Indeed, the latter were considered to be a good proxy for the incidence rates, which were not adequately recorded, due to poor prognosis after diagnosis during the follow-up of the LSS cohort members (NRC 2006).

Prediction of cancer risks in the target population

Measures of risk

Lifetime attributable risk (LAR) was defined as the cumulative excess risk potentially induced by any single CT examination, of developing a primary cancer from age at exposure e to a given attained age a . For each cancer site c , gender g , age at exposure e , attained age a , and organ dose d , the following formulation, noted $LAR^c(g, e, a, d)$, was derived from Kellerer et al. (2001) and Vaeth and Pierce (1990):

$$LAR^c(g, e, a, d) = \frac{1}{DDREF} \int_e^a F_{lag}^c(t - e) M^c(g, e, t, d) S(g, a_{min} = e, t) dt$$

$LAR^c(g, e, a, d)$ denotes the integral over attained ages $t = e$ through $t = a$ ($a = 100$ or $a = e + 25$ afterward) of excess risks noted $M^c(g, e, t, d)$ and defined as the following weighted arithmetic mean:

Table 1 Excess relative (ERR) and absolute (EAR) risk models, maximum likelihood estimates and associated 95 % confidence intervals (CIs) used for predicting potential risks of radiation-induced cancers

Breast cancer (women only) (Preston et al. (2002) model)	
$EAR(e, a, d).PY^{-1} = \beta.d.exp[\delta.(e - 25)].(a/50)^\gamma$	
$\beta = 9.9$	(7.1; 14.0)
$\delta = -0.040$	(-0.051; -0.028)
$(a < 50) \gamma_1 = 3.5$	(2.4; 4.9)
$(a \geq 50) \gamma_2 = 1.1$	(-0.4; 2.4)
Thyroid cancer (model derived from Ron et al. (1995) and NIH (2003) estimations)	
$ERR(g, e, d) = \beta.d.exp[\Theta.g + \delta.e]$	
$\beta = 9.449$	(3.937; 22.800)
$\delta = -0.083$	(-0.119; -0.046)
$\Theta = 0.346$	(-0.035; 0.715)
$g = -1$ for male, 1 for female	
Brain/CNS cancer (estimations from the models proposed by Preston et al. (2007) fitted to the LSS data (Preston et al. 2007))	
$ERR(e, d) = \beta.d.exp[\delta.[e/25]]$	
$\beta = 2.493$	(0.550; 13.680)
$\delta = -2.304$	(-18.950; -0.147)
$EAR(d).10^{-4} PY = \beta.d$	
$\beta = 0.508$	(0.120; 1.037)
Leukemia [estimations from the models proposed by UNSCEAR (2006) fitted to the LSS data (Ozasa et al. 2012)]	
$ERR(a, d) = (\alpha.d + \beta.d^2).exp[\gamma.ln[a/50]]$	
$\alpha = 1.612$	(0.124; 3.558)
$\beta = 1.551$	(0.621; 2.579)
$\gamma = -1.634$	(-2.419; -0.956)
$EAR(g, e, a, d).10^{-4}PY = (\alpha.d + \beta.d^2).exp[\Theta.g + \gamma.ln[(a - e)/25]]$	
$\alpha = 0.972$	(0.088; 1.982)
$\beta = 0.921$	(0.3495; 1.557)
$\gamma = -0.488$	(-0.856; -0.129)
$\Theta = -0.258$	(-0.464; -0.032)
$g = -1$ for male, 1 for female	

The brain/CNS cancer and leukemia models were here specified as in the original reports (Preston et al. 2007; UNSCEAR 2006) but fitted on centered data to facilitate computation of LRT-based CIs e age at exposure (in years), a attained age (in years), g gender, d organ dose (Gy), PY person-year, CNS central nervous system

$$M^c(g, e, t, d) = \omega_{ERR}ERR^c(g, e, t, d)\lambda^c(g, t) + (1 - \omega_{ERR})EAR^c(g, e, t, d)$$

where $\lambda^c(g, t)$ is a cancer-specific incidence rate at zero dose, gender g , and attained age t ; $ERR^c(g, e, t, d)$ and $EAR^c(g, e, t, d)$ quantify, respectively, the proportional and additional impact in the cancer risk (at cancer site c) for gender g , age at exposure e , and attained age t in response to an organ dose d ; ω_{ERR} is a weighting parameter between 0 and 1 to account, to some extent, for uncertainty in the dose–response model in population-to-population risk projection; F_{lag}^c is a

cancer-specific sigmoid function to describe a smoothed increase in excess cancer risk during a conventional latency period (Kocher et al. 2008; Berrington de Gonzalez et al. 2012); $S(g, a_{\min} = e, t)$ is the gender-specific survival probability: it denotes the conditional probability in the unexposed population alive at the age at exposure e of reaching at least age t cancer-free (Kellerer et al. 2001); the dose and dose-rate effectiveness factor (DDREF) proposed by the International Commission on Radiological Protection (ICRP) (ICRP 2005) is applied here to correct some potential bias induced when extrapolating excess risks under the linear dose–response relation assumption through dose ranges from those of the datasets used for fitting the models to the lower doses of the simulated CT exposures. No DDREF was considered for extrapolation from the linear-quadratic models of leukemia risk, which already describes a curvature in the dose–response relation.

To allow realistic comparisons with cancer risks in individuals not exposed to CT, the lifetime fractional risk (LFR) (Kellerer et al. 2001) was also calculated as follows:

$$\text{LFR}^c(g, e, a, d) = \frac{\text{LAR}^c(g, e, a, d)}{\text{LBR}^c(g, a_{\min} = e, a)}$$

where $\text{LBR}^c(g, a_{\min}, a)$ is the cancer- and gender-specific lifetime background risk (LBR) of primary cancer incidence, over a specific life period from the age a_{\min} (set at e for the LFR calculation) to an attained age a , in individuals unexposed to CT scans (Vaeth and Pierce 1990):

$$\text{LBR}^c(g, a_{\min}, a) = \int_{a_{\min}}^a \lambda^c(g, t) S(g, a_{\min}, t) dt$$

Gender-averaged excess and background risks were calculated as mean predictions for both genders weighted by sex ratios at each age.

Finally, overall cumulative excess and background risks were predicted in simulated populations exposed to repeated CT examinations during childhood and supposed to have the same demographic and exposure characteristics as the target population. $\text{LAR}_{\text{pop}}^c$ is then a cumulative excess risk of cancer incidence among individuals followed from their birth for P years and undergone one or more CT examinations before the age of 10 years:

$$\text{LAR}_{\text{pop}}^c = \sum_{i=1}^N \sum_{k=1}^{m_i} \text{LAR}^c(g_i, e_{ik, a=P, d_{ik}})$$

where N is the total number of individuals in the simulated population, m_i is the number of CT scans undergone by the individual i ($i = 1, \dots, N$), set here at the average number of CT scans per child in the target population (i.e., $m_i = 1.5$) for all i ; P is the total duration of follow-up of the population from birth (including the 10-year exposure period);

$\text{LAR}^c(g_i, e_{ik, a=P, d_{ik}})$ denotes the cumulative excess risk potentially induced by the k th CT examination—undergone by the child i and related to a specific organ dose d_{ik} —of developing a primary cancer c from age at exposure e_{ik} to attained age a at the end of the time of follow-up P ($P \geq e_{ik}$ for all $i = 1, \dots, N$ and $k = 1, \dots, m_i$). Excess risks of solid cancer were here predicted only from the examinations leading to direct exposure to the organ or tissue for which the site of cancer was of interest; risks of leukemia were assumed to be potentially induced by all the types of CT considered.

The total number of (background and excess) incident cases of cancer, noted C_{pop}^c , that could be observed in the exposed simulated population was predicted as a realization of Poisson’s distribution with mean and variance both equal to the sum of $\text{LAR}_{\text{pop}}^c$ and $\text{LBR}_{\text{pop}}^c$ where

$$\text{LBR}_{\text{pop}}^c = \sum_{i=1}^N \text{LBR}^c(g_i, a_{\min} = 0, a = P)$$

Predicted standardized incidence ratios (SIRs), noted $\text{SIR}_{\text{pop}}^c$, were then derived as ratios between C_{pop}^c and the “expected” number of incident cases of cancer c in the French general population, considered here as unexposed. This expected number of cancers was approximated by the $\text{LBR}_{\text{pop}}^c$, which is the sum over N individuals of the age- and gender-specific background rates of incidence of the general population, weighted by the cancer-free survival function $S(g, a_{\min} = 0, t)$. From the predicted C_{pop}^c and $\text{SIR}_{\text{pop}}^c$, the power to detect statistically significant $\text{SIR}_{\text{pop}}^c$ in the simulated population and the minimal detectable true value of SIR were calculated under the assumption that C_{pop}^c follows Poisson’s distribution with mean and variance both equal to $\text{LBR}_{\text{pop}}^c$ under the null hypothesis of SIR equal to 1 (Breslow and Day 1987).

Characterization and propagation of uncertainties

Prediction in the target population of all the above measures of cancer risk (i.e., $\text{LAR}^c(g, e, a, d)$, $\text{LBR}^c(g, a_{\min}, a)$, $\text{LAR}_{\text{pop}}^c$, etc.) took into account the variability of the inputs (i.e., organ doses, cancer incidence, and mortality rates) and the uncertainty in each radiation-induced cancer risk model parameter following the large-sample frequency properties of the Bayesian statistics and implicitly assuming a uniform prior density on each parameter (Gelman et al. 2004).

- Organ dose variability—For each type of CT and age group, the variability of the organ doses was characterized by the empirical distribution in the target population over the radiological protocols. For each organ or tissue, a single dose value (not necessarily different from one protocol to another) was computed by protocol (i.e., for specific type of CT, patient’s age

group, hospital, and period); the distributions of organ dose were then discrete.

- Background rate variability—The number of background incident cancers and deaths were assumed to follow Poisson's distribution with mean and variance both equal to the average French incidence and mortality rates over the period 2000–2005.
- Latency period—From an approach applied elsewhere (Kocher et al. 2008; Berrington de Gonzalez et al. 2012), the minimal latency period was characterized by a site-specific sigmoid function $F_{\text{lag}}^c(t - e)$ of the time after exposure necessary for expression of a potential radiation-induced effect:

$$F_{\text{lag}}^c(t - e) = \frac{1}{1 + \exp(-(t - e - \theta^c)/S^c)}$$

where θ^c is the time since exposure ($t - e$) at the inflection point (i.e., where the function equals 0.5) and S^c is the shape parameter that defines the steepness of the function. θ^c was defined here as the usual minimal latency time, i.e., for instance, 2 years for leukemia. S^c was defined such that the above sigmoid function attained 0.99 at the minimum time after exposure for which a significant excess risk has been shown in relevant epidemiological studies. For breast cancer, however, an appropriate latency period was defined on goodness-of-fit criteria (Land et al. 2003). The above sigmoid function reached the values 0.50 and 0.99, respectively, at the following times from exposure: for cancers of the brain/CNS, 5 and 9.5 years (Neglia et al. 2006; Pettorini et al. 2008), of the breast, 10 and 15 years (Preston et al. 2002; Land et al. 2003), of the thyroid, 3 and 4 years (Cardis et al. 2006; Cardis and Hatch 2011), and for leukemia, 2 and 3.5 years (Cardis et al. 2006; NRC 2006; UNSCEAR 2006). The uncertainty for each site-specific inflection point θ^c was characterized by Beta–Pert distributions with the following minimal, modal, and maximal values: for cancers of the thyroid, 2.5, 3, 3.5, of the breast, 9.5, 10, 12, and of the brain/CNS 2.5, 5, 7.5, and for leukemia, 1.5, 2, and 2.5.

- High-to-low doses risk extrapolation—Uncertainty in the DDREF, applied for only solid cancers, was characterized by the lognormal density function (mean = $\log(1.5)$, SD = 0.09) estimated by the BEIR committee (NRC 2006).
- Population-to-population risk transport—For leukemia and brain/CNS cancer, average lifetime risks were predicted following weighted arithmetic means of LAR^c from additive and multiplicative models. The weight for the relative risk transport (noted w_{ERR}) was assumed to follow a Bernoulli distribution with mean = 0.7 (NRC 2006). The w_{ERR} for breast cancer was equal to 0 and for thyroid cancer, 1 (see Table 1).
- Model parameters—The LSS and medically exposed population datasets were considered large enough that

it could be reasonably assumed that, given such data, the uncertainty distribution in most parameters followed an independent normal distribution centered at the maximum likelihood estimate (MLE) and with a standard error (SE) derived from the 95 % CI based on the likelihood ratio test (LRT). Exceptions were for the risk coefficient β of the breast cancer model and the parameters of the ERR model for CNS/brain cancer (see Table 1) for which the asymptotic normality seemed to be improved by log transformation (Gelman et al. 2004), and thus independent lognormal distributions were assumed. For thyroid cancer, the empirical distribution of the MLE for each parameter β and δ was first assessed by making several linear interpolations of sets of random values of $\log(\text{ERR})$ simulated from normal distributions with means equal to each point estimate of $\log(\text{ERR})$ (by increments of 5 years of exposure) and SEs both estimated by the NIH (2003). This allowed to derive the expected MLE and a 95 % CI for each parameter β and δ (Table 1). Then, the uncertainty distributions for those parameters were assumed to follow independent normal distributions centered at the corresponding expected MLEs and with a SE equal to the empirical SE of the MLE. The uncertainty distribution for gender effect θ was derived from the OR between genders to which we assigned a lognormal distribution with a mean equal to $\log(\text{MLE})$ and a SE derived from the two-sided score test p value (Ron et al. 1995). Considering an asymptotically equivalent Wald test, we estimated that $\text{OR}_{\text{male:female}} = 0.50$ 95 % CI [0.24;1.07].

Uncertainties in all the above parameters and variability in the inputs were propagated through the dose–response models and the risk measures by standard Monte Carlo simulations (Phillips 2003) to derive uncertainty distributions of the outcomes of interest: the predicted cancer risks by type of CT and for each gender, age at exposure, and site of cancer. Basically, 10,000 random sets of values for inputs and parameters were generated with WinBUGS 1.4 (Lunn et al. 2000), here used as a simulation tool, to provide an empirical uncertainty distribution of the predicted cumulative excess (and background) risks of each cancer.

Results

Description of the CT exposures in the target population

Between 2004 and 2009, 65,675 children younger than 10 years underwent 105,558 CT scans in the 15 participating hospitals; 24.5 % of the examinations were in

Table 2 Number of radiological protocols and computed tomography (CT) examinations and summary statistics of the empirical distributions of organ doses from CT examinations in the target population of children exposed before the age of 10 years

CT type	Number of radiological protocols (hospitals) ^a	Number of examinations	Median, minimum–maximum organ dose (mGy) according to age at examination							
			<1 year				1–10 years			
			Bone marrow	Brain	Thyroid	Breasts	Bone marrow	Brain	Thyroid	Breasts
Skull/brain	27 (15)	49,024	6 2–15	21 8–55			4 1–8	27 6–56		
Middle ear	22 (13)	5,503	8 2–14	18 4–29			2 1–6	9 2–20		
Cervical spine	9 (7)	3,521	8 1–10		28 3–36		3 1–3		21 6–22	
Chest	27 (15)	23,018	2 1–6		8 3–25	8 2–23	1 <0.5–4		7 3–25	7 3–25
Abdomen +pelvis	27 (15)	6,849	2 1–4				3 1–4			2 1–10

^a Each radiological department (hospital) drew up one radiological protocol for a defined anatomical area, a CT machine and a given use period according to the patients' age (or body weight) class

children younger than 1 year old and 42.4 % in girls. The five types of CT of interest here accounted for 84.5 % of the 100,332 examinations for which the anatomical area imaged was known: 57.9 % scans were of the skull/brain, 6.5 % the middle ear, 4.2 % the cervical spine, 27.2 % the chest, and 8.1 % the abdomen + pelvis (one examination could involve several anatomical areas).

Table 2 describes the organ doses by CT type and age group at examination. For given CT type and age group, the ratio between the highest and the lowest doses ranged from 3 to 15 and was about 10 in most cases.

Lifetime cancer risk attributable to a single CT examination

Table 3 presents summary statistics of the predictive distributions obtained for the gender-averaged LBR^c and LAR^c values by age at exposure and type of CT. Because the LBR^c values were essentially equivalent whether measured from age 1 month or age 10 years through age 100, only estimations from birth are shown. For all types of CT, the predictive medians of LAR^c were highest for the youngest ages at exposure and the width of the associated 90 % UIs decreased along with age at exposure. For leukemia and brain/CNS cancer, the LAR^c were similar between genders despite differences in background risks (Online Resource 1—Suppl. Table 2 gives LBR^c and LAR^c to age 100 by gender). For thyroid cancer, however, the LAR^c were 6–7 times higher in females than those in males. For instance, chest scans in 5-year-olds would lead to LBR^c and LAR^c of thyroid of 1,189 (90 % UI 1,136–1,242) and 51 (90 % UI 15–175) $\times 10^{-5}$,

respectively, in females, and 371 (90 % UI 344–400) and 8 (90 % UI 2–27) $\times 10^{-5}$, respectively, in males. In comparison with LBR^c, the potential excess risks of thyroid cancer were then twice as high for females, whatever the time since exposure (see the values of LFR^c in Online Resource 1—Suppl. Tables 3 and 4).

Figure 1 displays the gender-averaged LAR^c per 100,000 children exposed to one CT examination at age 5, and LFR^c per 1,000 background cancers from age at exposure 5 to 100 year -old (Online Resource 1—Suppl. Table 4 shows values of LFR^c to age 100 by gender and age at exposure). It illustrates the decrease in LFR^c, though increase in LAR^c, with attained age, with different shapes for each cancer site due to the increase in the background risks, while the potential radiation-induced risks either remained constant or decreased with attained age or time since exposure after the latency period. A purely multiplicative risk model for thyroid cancer, not dependent on time since exposure, would result, however, in a constant LFR^c throughout life.

Cumulative excess risks of cancer 20 years after a single CT examination

Table 4 presents summary statistics of the predictive distribution of gender-averaged LAR^c per 100,000 children exposed to one CT examination at 5 year old (see Online Resource 1—Suppl. Table 1 for other ages at exposure) and gender-averaged LFR^c per 1,000 background cancers (if unexposed to CT), 20 years after a CT exposure. Although the LAR^c were lower at 20 years after a CT examination than throughout life, they were highest

Table 3 Predictive medians and associated 90 % uncertainty intervals of gender-averaged lifetime background risks (LBR^c) of primary cancers incidence, from birth to age 100, per 100,000 unexposed

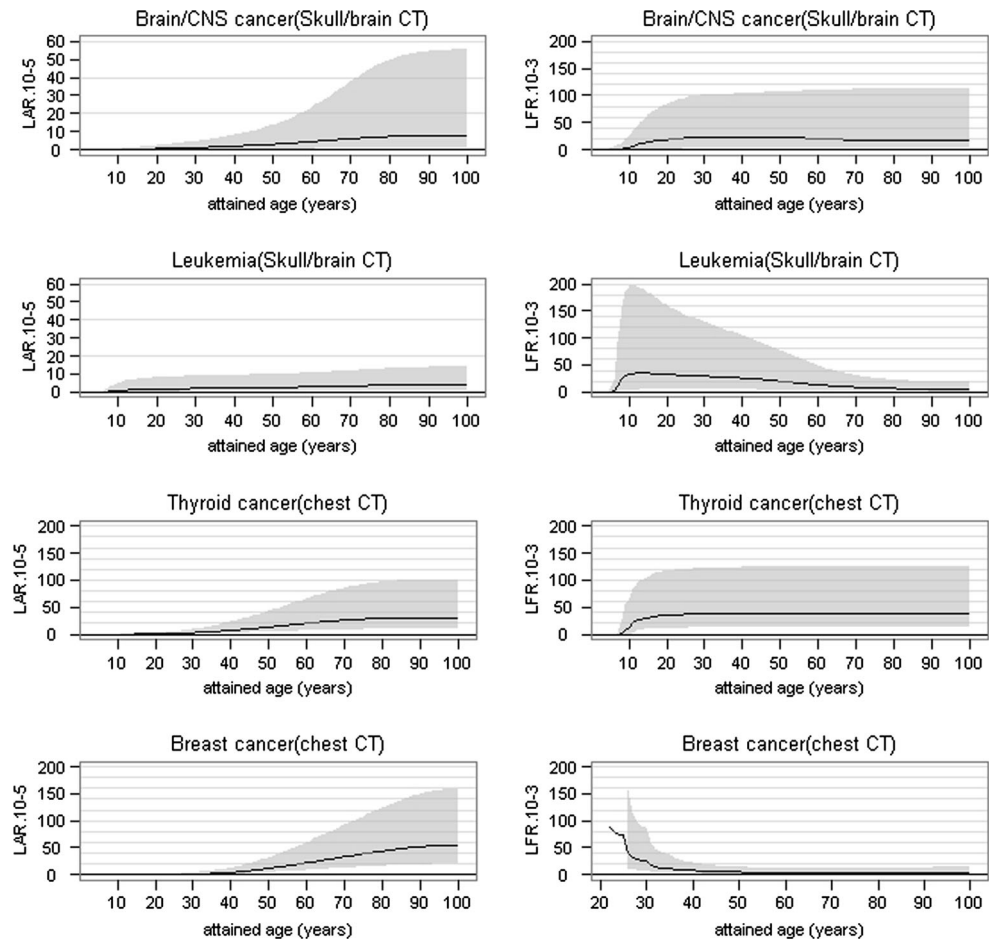
children, and gender-averaged lifetime attributable risks (LAR^c) per 100,000 children exposed to one computed tomography (CT) examination by type of CT, from several ages at exposure to age 100

CT type from birth to age 100	Site of cancer <i>c</i>	LBR ^c × 10 ⁻⁵	LAR ^c × 10 ⁻⁵ to age 100 according to age at exposure			
			1 month	1 year	5 years	10 years
Skull/brain	Brain and CNS	500 (478–522)	12 (2–83)	11 (2–73)	8 (1–55)	6 (0.2–41)
	Leukemia	779 (754–806)	17 (1–138)	13 (1–82)	4 (1–14)	3 (0.5–9)
Middle ear	Brain and CNS	500 (478–522)	8 (2–55)	7 (1–48)	2 (0.3–18)	2 (<0.1–13)
	Leukemia	779 (754–806)	16 (1–150)	13 (1–87)	2 (0.4–9)	2 (0.3–6)
Cervical spine	Thyroid	800 (769–830)	152 (26–474)	141 (24–440)	65 (17–196)	43 (11–134)
	Leukemia	779 (754–806)	17 (1–140)	13 (1–82)	3 (0.4–8)	2 (0.4–5)
Chest	Thyroid	800 (769–830)	46 (12–158)	43 (12–146)	31 (9–101)	20 (6–69)
	Breast ^a	11,380 (11,240–11,530)	62 (17–173)	60 (17–167)	55 (20–158)	45 (16–129)
	Leukemia	779 (754–806)	5 (0.4–41)	4 (0.4–25)	1 (<0.1–4)	1 (<0.1–2)
Abdomen + pelvis	Breast ^a	11,380 (11,240–11,530)	36 (7–107)	35 (7–103)	17 (5–79)	14 (4–64)
	Leukemia	779 (754–806)	5 (0.4–38)	4 (0.4–22)	3 (0.4–9)	2 (0.4–5)

CNS central nervous system

^a In girls only

Fig. 1 Gender-averaged lifetime attributable risks (LAR^c) of cancer *c* incidence per 100,000 children exposed to one computed tomography (CT) examination at the age of 5 years (*left*) and gender-averaged lifetime fractional risks (LFR^c) per 1,000 background cancers (*right*), from age at exposure to 100 year old in a cancer-free population, for the most frequent CT types. *Black lines* represent the predictive medians of LAR^c and *gray areas* the associated 90 % uncertainty intervals. CNS central nervous system



relative to the background risks in the first decades after exposure, except for thyroid cancer, as illustrated also in Fig. 1 (see the LFR^c). In contrast to LAR^c to age 100, the

cumulative excess risks of thyroid and breast cancer at 20 years after exposure increased slightly with age at exposure due to the strong increase in the background risks

Table 4 Predictive medians and associated 90 % uncertainty intervals of gender-averaged lifetime attributable risks (LAR^c) of primary cancers incidence per 100,000 children exposed to one computed tomography (CT) examination at the age of 5 years and gender-averaged lifetime fractional risk (LFR^c) of primary cancers incidence per 1,000 background cancers, by type of CT and age at exposure, 20 years after CT exposure

CT type	Site of cancer <i>c</i>	LAR ^c × 10 ⁻⁵	LFR ^c × 10 ⁻³ 20 years after exposure by age at exposure			
			1 month	1 year	5 years	10 years
Skull/brain	Brain and CNS	1 (0.1–3)	29 (6–126)	25 (4–109)	21 (2–95)	17 (0.3–87)
	Leukemia	2 (0.2–9)	165 (8–1,748)	111 (7–960)	31 (4–144)	23 (4–68)
Middle ear	Brain and CNS	0.2 (<0.1–1)	19 (3–84)	17 (3–71)	7 (0.5–32)	5 (0.1–28)
	Leukemia	1 (0.2–6)	162 (7–1,877)	109 (7–1022)	18 (3–94)	13 (2–46)
Cervical spine	Thyroid	3 (1–8)	183 (31–568)	169 (29–529)	78 (20–236)	51 (13–160)
	Leukemia	1 (0.2–5)	159 (5–1,772)	107 (4–961)	19 (3–84)	14 (3–39)
Chest	Thyroid	1 (0.4–4)	56 (15–188)	52 (14–174)	37 (11–120)	24 (7–82)
	Breast ^a	0.5 (0.1–2)	583 (41–nc)	148 (24–nc)	75 (19–332)	18 (6–60)
	Leukemia	0.5 (<0.1–2)	50 (2–528)	33 (2–290)	8 (<0.1–38)	6 (<0.1–19)
Abdomen + pelvis	Breast ^a	0.2 (<0.1–0.9)	345 (18–nc)	86 (10–nc)	25 (5–162)	6 (1–30)
	Leukemia	1 (0.2–5)	50 (2–480)	34 (2–266)	20 (3–90)	14 (3–42)

CNS central nervous system, *nc* not computed because lower bound of cumulative background risk of breast cancer incidence was 0 before the age of 22 years

^a In girls only

from the age of 25 and even more from 30 years (Online Resource 1—Suppl. Table 1). No such trend was observed for either leukemia or CNS/brain cancer, for which the annual incidence rates remained essentially constant for all ages.

Variability of lifetime excess risk across the radiological protocols

Figure 2 shows gender-averaged LAR^c from age at exposure 5 to age 100 per 100,000 children (y-axis) in relation to the cumulative frequency, in the target population, of skull/brain or chest CT examinations associated with the given organ doses for which the LAR^c were predicted (x-axis). It illustrates the variability in potential excess risks, for a given CT type, subsequent to dose variability in the target population. In particular, while 50 % of the 5-year-old girls who had one chest scan would have been subjected to a LAR^c of breast cancer equal to or <54 (90 % UI 27–109) × 10⁻⁵, 5 % of them received a dose associated with a potential excess risk equal to or more than 124 (90 % UI 63–249) × 10⁻⁵. The LAR^c of thyroid cancer similarly varied from <30 (90 % UI 11–76) × 10⁻⁵ for 50 % of the children exposed to one chest scan to 68 (90 % UI 26–173) × 10⁻⁵ or more for the 95th percentile. Uncertainties in predictions did not allow to highlight the risk variability for brain/CNS cancer and leukemia as clearly, but the dose ranges between the radiological protocols were also wide (Table 2).

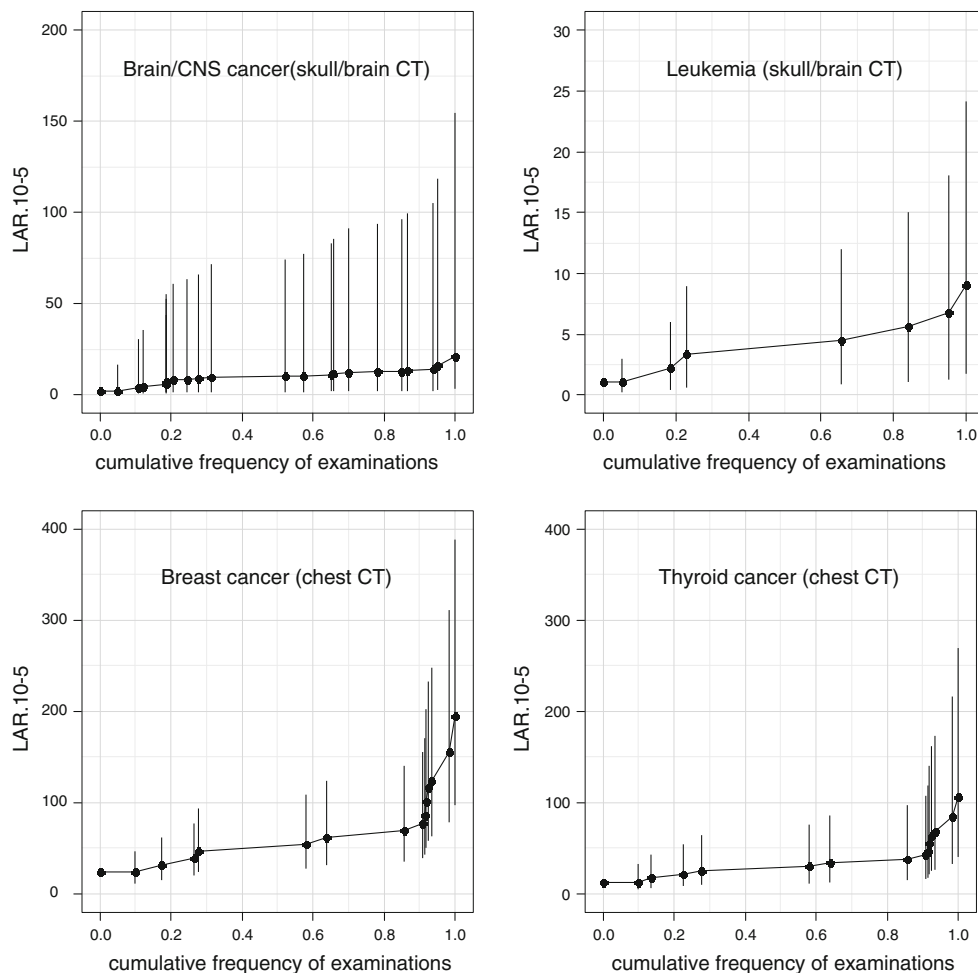
Overall cancer risks in populations having childhood CT examinations

Table 5 reports the predicted total (background and excess) number of incident cases of cancer that would be observed when following simulated exposed population, assuming the demographic and exposure characteristics of the target population, the power to detect SIR_{pop}^c >1, and the minimal detectable true value of SIR according to survey scenarios. In a fictitious population of 100,000 exposed individuals, the power to detect significant SIR_{pop}^c was 20 % for leukemia and thyroid cancer by 20 and 50 years of follow-up, respectively, but would not exceed 10 % for CNS/brain and breast cancers even through 50 years of follow-up. Following such a population of one million individuals made a power of 80 % achievable for leukemia and thyroid cancer. For CNS/brain and breast cancer, a low performance was once more predicted, but the minimal detectable SIR decreased notably with increasing the duration of follow-up.

Discussion

Risk predictions here describe the potential radiation-induced risks of cancer specifically from standard CT scans in pediatrics. The QRA approach applied emphasizes that, although the potential lifetime excess risks induced by childhood CT were expected to be low, they would be noticeable during the first decades of life in comparison

Fig. 2 Gender-averaged lifetime attributable risks (LAR^c) of cancer c incidence per 100,000 children exposed at 5 years of age to one examination of the most frequent types of computed tomography (CT) according to the cumulative frequency in the target population of such examinations associated with a given organ dose. For each specific value of organ dose d in the target population (related to one or several radiological protocols) from examinations at 5 years of age, the y -axis presents the associated predictive gender-averaged median of LAR^c (black points) and 90 % uncertainty intervals (vertical lines), and the x -axis indicates the cumulative frequency of such examinations associated with an organ dose less or equal to d . CNS central nervous system



with the background risks which remain low (Table 4; Fig. 1). In addition, the excess risks to children with scans at the age of 1 year could be 1.3–2.5 times higher for breast cancer and 2–3 times higher for thyroid cancer, compared with children exposed at the same doses at the age of 10 years (Table 3). On the whole, the results showed that 11 and 2 excess thyroid cancers, respectively, would be induced by 10,000 cervical spine examinations in 5-year-old girls and boys (i.e., 1 radiation-induced cancer in 1,500 scans for both genders, see Online Resource 1—Suppl. Table 5). Chest CT would lead to risks of breast cancer similar to those of thyroid cancer in females—about 6 excess cases per 10,000 scans in 5-year-old girls (i.e., 1 in 1,800 scans). The risk of breast cancer from abdominal imaging would be only one half to one-third the risk from chest CT (i.e., 1 in 2,800–7,100 scans according to age at exposure). The risk of brain/CNS tumors from head CT would be low (2–12 per 100,000 according to age at examination), but the frequency of these examinations (Table 2) might induce a noticeable collective impact. Despite the low doses, 1–5 cases of radiation-induced leukemia per 100,000 scans would occur in children

exposed at the age of 5 years, regardless of the CT type, and those risks would be substantially higher in younger children. These results must nevertheless be interpreted cautiously in view of the acute uncertainty in the estimation of the bone marrow doses due to diffused exposure (Lechel et al. 2009). Slight differences between genders were predicted in excess risks of leukemia and brain/CNS cancer. For thyroid cancer, however, the background and radiation-related risks, each about twice as high for females than males, implied a substantially higher excess risk for girls exposed to CT who would have, moreover, a longer life expectancy (Tables 1 and 3).

Previous major risk assessments for CT exposure (Brenner et al. 2001; Berrington de Gonzalez and Darby 2004, 2009; Brenner and Hall 2007; Chodick et al. 2007; Smith-Bindman et al. 2009) have focused mainly on the risks of incidence of all cancers or cause-specific mortality for all ages at exposure. The present work aimed, on the contrary, at predicting cancer risk according to the characteristics of childhood exposures, and targeted the cancer sites which would appear as relevant for predicting the incident cases that could occur in the reference

Table 5 Medians and associated 90 % uncertainty intervals of predicted numbers of incident cancers (C_{pop}^c) in fictitious populations of individuals exposed to CT examinations before the age of 10 years, medians of predicted standardized incidence ratios (SIR_{pop}^c) and the

associated power to detect significant differences to 1 at the 0.05 level, and minimal detectable SIR with a power of 80 %, according to the size and the duration of follow-up of the simulated exposed population

Site of cancer	Survey duration (in years)	C_{pop}^c	SIR_{pop}^c	Power (%) to detect $SIR_{pop}^c > 1$	Minimal detectable SIR with power of 80 %				
					Size of the exposed population ($\times 10^5$)				
					10	1	10	1	10
CNS/brain cancer	10	212 (156–274)	1.01	4	7	1.65			1.18
	20	368 (292–450)	1.02	6	9	1.47			1.14
	30	570 (472–677)	1.03	7	16	1.37			1.11
	50	1,428 (1,275–1,617)	1.03	10	29	1.23			1.07
Leukemia	10	564 (447–906)	1.10	17	70	1.39			1.11
	20	818 (676–1,192)	1.09	22	84	1.33			1.09
	30	1,010 (853–1,374)	1.09	22	85	1.29			1.08
	50	1,599 (1,409–1,979)	1.06	18	74	1.21			1.07
Thyroid cancer	10	16 (3–36)	1.01	2	5	4.30			1.73
	20	133 (90–183)	1.05	5	14	1.86			1.23
	30	683 (576–800)	1.05	11	34	1.34			1.10
	50	3,293 (3,033–3,625)	1.05	21	86	1.15			1.04
Breast cancer	10	0 (0–0)	–	–	–	–			–
	20	7 (0–27)	1.01	2	5	5.60			1.94
	30	469 (357–589)	1.01	5	8	1.41			1.12
	50	22,990 (22,210–23,800)	1.00	6	9	1.05			1.02

CNS central nervous system. The exposed population was considered here as individuals undergone one or more CT scans whatever the type of examination. Cumulative doses (mGy) to brain, bone marrow, thyroid gland, and breast (in girls only) per individual were 24 (13–36), 6 (4–8), 8 (4–11), 4 (2–8), respectively. Survey duration is the total duration of follow-up from birth to the end of the survey (it thus includes the 10-year period of exposure). Power to detect $SIR_{pop}^c > 1$ and minimal detectable SIR are related to the median values of SIR_{pop}^c and C_{pop}^c , respectively, and derived from one-sided exact tests with $\alpha = 0.05$ and the usual assumption that, under the null hypothesis of $SIR = 1$, the observed number of incident cancers, predicted as, is Poisson distributed with mean and variance both equal to the “expected” number of cancers in the general population (Breslow and Day 1987), approximated here by the LBR_{pop}^c

population—the *Enfant Scanner* cohort. Our predictions are therefore in most cases not directly comparable to the previous estimations. Brenner and Hall (2007) nevertheless reported, based on other risk models, slightly higher potential excess risks of leukemia mortality from head CT at 5–10 years of age for organ doses similar to those considered here, and similar risks from abdominal CT despite higher doses. QRA for all-cancer incidence as a single endpoint attributable to head CT scans have, however, yielded substantially higher risk predictions than those we could obtain by adding predicted risks of leukemia and brain/CNS cancer (Berrington de Gonzalez et al. 2009; Smith-Bindman et al. 2009).

In our view, targeted exposure to specific organs and limitations of models for all cancers and for some rare cancers did not allow, however, relevant predictions for providing a single measure of the risk of all cancers. Unlike previous predictions, the current risk assessment focused here on cancer sites for which significant associations have been shown and consistent estimations provided

across several studies (breast and thyroid cancers). The potential risk of leukemia was also studied because of its strong association with the exposure of bone marrow to IR (Preston et al. 2004; Wakeford 2013), and intracranial cancers because pediatric CT involves mainly head examinations (Etard et al. 2010; Bernier et al. 2012b) even though the estimated risk models involve large degrees of uncertainty. These four cancer sites contribute to approximately 50 % of women’s and 5 % of men’s overall lifetime risk of cancer in the French general population (Belot et al. 2008). Prostate, colon, and lung cancers play a major role in the background risk, especially among men, but there is not yet sufficient evidence that IR affects prostate cancer (UNSCEAR 2006; Ozasa et al. 2012), pelvic CT was not frequent in children (Bernier et al. 2012b), and it would be difficult to predict the impact of tobacco intake on the relation between lung cancer and IR (Furukawa et al. 2010). A more complete overview of the potential risks associated with frequent types of CT in children will require taking into account other cancer sites, particularly

lung, liver, gastrointestinal tract, and skin (other than melanoma), based on an appropriate characterization of the dose–response relations and of the absorbed doses to the tissues.

The current QRA aimed to assess the magnitude of potential cancer risks from routine CT examinations in children without underlying conditions likely to reduce their cancer-free life expectancy. This limitation is related to the estimation of the cancer-free survival in the unexposed target population from which the excess risks were predicted. Although one can appropriately consider that the general population was almost entirely unexposed to CT in childhood (Etard et al. 2012), specific clinical conditions that result in CT imaging may well modify the children's probability of cancer-free survival (unknown in the current state of knowledge) in comparison with children who never receive such medical care, regardless of the potential effects of CT radiation. Thus, the probability of survival and of subsequent potential risks from CT radiation might be somewhat overestimated for some exposed children. The radiation-induced risks are otherwise not of significant concern for children at high risk of death due to their primary clinical conditions (Brenner et al. 2011). Thanks in part to improved diagnoses and medical monitoring by high-quality radiological imaging, many children who underwent CT scans might nonetheless have a long cancer-free life expectancy. Although specific mortality risks for them are difficult to assess, the high primary risk of cancer related to the underlying medical conditions likely concerns only a small percentage of the exposed patients (Hammer et al. 2009; Bernier et al. 2012a).

In a step beyond that of previous works on this topic, in the present work, current practices in routine care in pediatrics were taken into account in predicting lifetime cancer risks potentially induced by CT scans. The empirical organ dose distribution in the target population can be viewed as representative of radiological practices in French University hospitals during the survey period: the facilities were among those with the highest volume of activity and represented a wide geographical area. The frequency of examinations per hospital varied from 1.5 to 10 %, while one hospital accounted for more than 20 %. Doses in that hospital were nevertheless similar to the median values in the other facilities. The empirical organ dose distributions for cervical spine CT was built, however, from the protocols available in only seven hospitals among which two facilities accounted for almost 70 % of the examinations. For this type of CT, the risk predictions were thus essentially based upon the protocols in use in the two mentioned radiological units and associated otherwise with the highest doses. Median (minimum–maximum) effective doses (mSv) from examinations in children aged 1–10 years were 1 (<0.5–3) for the skull/brain, 1 (<0.5–1) for the middle

ear, 2 (1–2) for the cervical spine, 3 (1–9) for chest scans, and 6 (2–12) for abdominal/pelvic CT scans. These results are similar to those from previous surveys in pediatric CT (McLean et al. 2003; Shrimpton et al. 2006).

Data from routine practices highlight here the variability in doses and thus in potential cancer risks across the radiological protocols implemented in 15 major hospitals in France. The predictive distributions of cancer risk did not, however, reflect uncertainties about the computational method for estimating organ doses and the inter-individual variability (related to the radiological parameters actually used at each examination and the heterogeneity in body and organ size compared with the characteristics of the phantoms used in the dose calculations) likely to explain some of this cross-protocol dose variability. We assumed that the dose values calculated for each protocol approximated the means of individual dose values for specific CT equipment, periods, and hospitals. Although these limitations on dose estimation led to an underestimation of the uncertainty in risk prediction, the results presented here show that 5–10 % of the examinations were carried out according to radiological protocols that resulted in much higher potential excess risks, 1.4–3.6 times higher than the 50th percentile of examinations. This variability in doses and subsequent potential cancer risks between the hospitals, resulting only from CT equipment and the specified technical parameters, suggests that the protocols for routine CT scans should be optimized to reduce doses.

Another important source of uncertainty in the QRA was the extrapolation of risk from the dose ranges in epidemiological studies to lower doses from simulated CT exposures and risk projection to the French population, which might have different background risks. The uncertainty factor applied to take into account the probability of a sublinear dose–response relation at low doses may lead to sizeable differences in risk predictions of solid cancers. If we had not applied any DDREF, the central estimations would indeed be 50 % higher and the UIs 20–35 % lower. In addition, a large uncertainty remained about the appropriate method for population-to-population risk transport, especially when the dose–response models were estimated from only one epidemiological dataset. The median values of LAR^c were here 2–10 times higher when we applied a multiplicative model at 10 mGy for predicting leukemia risks instead of considering an additive risk transport, and 1–4 times higher for CNS/brain cancer, depending on gender and age at exposure (Online Resource 2). Comparison of excess risks estimated from the LSS with those after repetitive exposures at high doses from radiotherapy has nevertheless supported the appropriateness of multiplicative risk transport, for leukemia at least, even though those medical studies do not yield results directly relevant for predicting risks from CT (Little 2001, 2008). Further,

the first results on risk of leukemia after CT exposures in childhood and early adulthood (Pearce et al. 2012; Mathews et al. 2013) reported consistent ERR estimates with the LSS data during the first years after exposure. At quite close level of exposure to CT, Karlsson et al. (1998) estimated also a risk of intracranial tumor incidence ($\text{ERR.Gy}^{-1} = 0.0027$ (95 % CI 0.0010–0.0056), mean follow-up 32 years) after radiotherapy for skin hemangioma (mean cumulative brain dose 70 mGy) in young children (0–7 years) consistent with that one we could estimate from the LSS dataset ($\text{ERR.Gy}^{-1} = 0.0042$ (95 % CI 0.0009–0.0131), mean follow-up 32 years) in children exposed before the age of 5 years up to 50 years after exposure. Other studies on risk of brain/CNS cancer after high-dose exposures (Shore et al. 2003; Sadetzki et al. 2005; UNSCEAR 2006; Schulze-Rath et al. 2008) or CT examinations (Pearce et al. 2012; Mathews et al. 2013), however, have produced very different estimates. In view of large uncertainties about the dose–response relation for CNS/brain cancer, a quantitative comparison of the available results may be worthwhile, particularly to better characterize the potential risks in children and infants for whom most data could be available.

Our study indicates a large degree of uncertainty attached to risk prediction, especially when multiplicative risk models were considered, that is, for leukemia, CNS/brain and thyroid cancers, and for the patients who were youngest at the time of examination. The characterization of uncertainties was nevertheless limited by subjective distribution assignments to the model parameters based on the results from specific contexts of exposure, as well as by uncharacterized measurement errors in dose estimation. Questions also remain about the modeling of the effects modifying the dose–response relation. For thyroid cancer, the risk prediction was based on a gender-specific risk coefficient, derived a posteriori from the results by Ron et al. (1995) and took the lack of significance of this parameter in the pooled analysis into account through the uncertainty analysis. The differences in central values of prediction risk between genders must nevertheless be interpreted very carefully as such a sex ratio was inconsistent in the original studies (Ron et al. 1995). Furthermore, assuming that the effects of gender and age at exposure were independent without validating the derived dose–response model against the unavailable original dataset may have led to use biased estimates for predicting excess risks according to characteristics at exposure. A previous QRA used another approach, based on the BEIR's methodology, for modeling the modifying effects of leukemia and CNS/brain cancer risks in the LSS (NRC 2006; Berrington de Gonzalez et al. 2012). The excess risks given at 10 mGy for the US population (Berrington de Gonzalez et al. 2012) were then mostly of a same order of magnitude

as those from the methodology presented here (the risk predictions at exposure of 10 mGy are given in Online Resource 2). Our predictions, as the attached uncertainties, were nevertheless higher up to 1 year of age at exposure for leukemia (+30–60 %), and also in females for CNS/brain cancer as we did not consider any effect of gender on radiation-induced risks.

Specific epidemiological studies on childhood CT exposures should result in better characterization of the radiation-induced cancer risk, especially in terms of the uncertainties in risk prediction from other contexts of exposure. Several nationwide cohorts are thus underway or continuing to follow children and young adults exposed to CT scans (Bernier et al. 2012b; Krille et al. 2011; Pearce et al. 2012). Based on the QRA assumptions, low overall relative risks would be predictable, from 1 to 10 % depending on the site of cancer we consider and the duration of follow-up (Table 5). As stated above, the predictive risk of leukemia was consistent with the estimates from studies on CT exposures [$\text{SIR}_{\text{pop}}^c = 1.09$ here vs incidence rate ratio (excluding myelodysplasias) = 1.19 (95 % CI 1.03–1.37) (Mathews et al. 2013)]. The uncertainties in prediction of observable numbers of cases, which we detail above, may nevertheless substantially modify the predictable powers to detect such excess risks. Accordingly, very large populations should be followed during extended periods to characterize accurately the dose–response relation for childhood exposures and to confirm or invalidate the usual assumptions for extrapolation of risks from the LSS and high-dose medical studies to low-dose exposures such as routine CT examinations. For this purpose, the International Agency for Research on Cancer has set up the European project Epi-CT (Thierry-Chef et al. 2013) to gather national cohorts in nine countries and provide powerful results.

While further epidemiological results from ongoing cohorts are awaited, the results from QRAs emphasize that the expected clinical benefits of CT scans should be considered in light of their potential lifetime adverse risks. This issue is of special concern in children because most have a long-life expectancy and potential radiation-induced risks of cancer related to pediatric examinations may not be negligible in comparison with the background risks in the first decades of life. In clinical practice, management of those potential risks should be supported by optimization of the radiological protocols for routine examinations.

Acknowledgments We are particularly grateful to the radiologists working in the participating hospitals (France) who provided us with information about the radiological protocols used in their department: Pr N Boutry (CHU de Lille), Pr F Brunelle (CHU Necker-Enfants-Malades-Paris), Pr JF Chateil (CHU Pellegrin-Bordeaux), Pr E Dion (CHU Louis Mourier – Colombes), Pr H Ducou Le Pointe (CHU Armand Trousseau – Paris), Dr S Franchi (CHU de Bicêtre), Dr MF

Galloy (CHU de Nancy), Pr JM Garcier and Dr J Guersen (CHU de Clermont-Ferrand), Pr G Khalifa (CHU Saint-Vincent de Paul – Paris), Dr D Loisel (CHU d’Angers), Pr D Musset (CHU Antoine Bécélère – Clamart), Pr D Pariente (CHU de Bicêtre), Pr P Petit (CHU de Marseille), Dr E Schmitt (CHU de Nancy), Pr G Sebag (CHU Robert Debré – Paris), Pr D Sirinelli (CHU Clocheville – Tours), Dr J Vial (CHU de Toulouse). We also thank Olivier Laurent (IRSN, France) very much for helpful discussions on methods at early stages of the work. This report makes use of data obtained from the Radiation Effects Research Foundation (RERF) in Hiroshima, Japan. RERF is a private foundation funded equally by the Japanese Ministry of Health, Labour, and Welfare and the US Department of Energy through the US National Academy of Sciences. The data include information obtained from the Hiroshima City, Hiroshima Prefecture, Nagasaki City, and Nagasaki Prefecture Tumor Registries and the Hiroshima and Nagasaki Tissue Registries. The conclusions in this report are those of the authors and do not necessarily reflect the scientific judgment of RERF or its funding agencies. This work was funded by *La Ligue contre le cancer* (PRE09/MOB) and the French National Cancer Institute (*INCa*) (2011-1-PL-SHS-01-IRSN-1).

References

- Adams MJ, Dozier A, Shore RE, Lipshultz SE, Schwartz RG, Constine LS, Pearson TA, Stovall M, Winters P, Fisher SG (2010) Breast cancer risk 55 + years after irradiation for an enlarged thymus and its implications for early childhood medical irradiation today. *Cancer Epidemiol Biomarkers Prev* 19(1):48–58
- Baysson H, Etard C, Brisse HJ, Bernier MO (2012) Diagnostic radiation exposure in children and cancer risk: current knowledge and perspectives. *Arch Pediatr* 19(1):64–73
- Belot A, Grosclaude P, Bossard N, Jouglu E, Benhamou E, Delafosse P, Guizard AV, Molinie F, Danzon A, Bara S, Bouvier AM, Tretarre B, Binder-Foucard F, Colonna M, Daubisse L, Hedelin G, Launoy G, Le Stang N, Maynadie M, Monnereau A, Troussard X, Faivre J, Collignon A, Janoray I, Arveux P, Buemi A, Raverdy N, Schwartz C, Bovet M, Cherie-Challine L, Esteve J, Remontet L, Velten M (2008) Cancer incidence and mortality in France over the period 1980–2005. *Rev Epidemiol Sante Publique* 56(3):159–175
- Bernier MO, Mezzarobba M, Maupu E, Caer-Lorho S, Brisse HJ, Laurier D, Brunelle F, Chatellier G (2012a) Role of French hospital claims databases from care units in epidemiological studies: the example of the “Cohorte Enfant Scanner” study. *Rev Epidemiol Sante Publique* 60(5):363–370
- Bernier MO, Rehel JL, Brisse HJ, Wu-Zhou X, Caer-Lorho S, Jacob S, Chateil JF, Aubert B, Laurier D (2012b) Radiation exposure from CT in early childhood: a French large-scale multicentre study. *Br J Radiol* 85(1009):53–60
- Berrington de Gonzalez A, Darby S (2004) Risk of cancer from diagnostic X-rays: estimates for the UK and 14 other countries. *Lancet* 363(9406):345–351
- Berrington de Gonzalez A, Mahesh M, Kim KP, Bhargavan M, Lewis R, Mettler F, Land C (2009) Projected cancer risks from computed tomographic scans performed in the United States in 2007. *Arch Intern Med* 169(22):2071–2077
- Berrington de Gonzalez A, Apostoaiei JA, Veiga LH, Rajaraman P, Thomas BA, Owen Hoffman F, Gilbert E, Land C (2012) RadRAT: a radiation risk assessment tool for lifetime cancer risk projection. *J Radiol Prot* 32(3):205–222
- Boice JD Jr, Preston D, Davis FG, Monson RR (1991) Frequent chest X-ray fluoroscopy and breast cancer incidence among tuberculosis patients in Massachusetts. *Radiat Res* 125(2):214–222
- Brenner DJ, Hall EJ (2007) Computed tomography—an increasing source of radiation exposure. *N Engl J Med* 357(22):2277–2284
- Brenner D, Elliston C, Hall E, Berdon W (2001) Estimated risks of radiation-induced fatal cancer from pediatric CT. *Am J Roentgenol* 176(2):289–296
- Brenner DJ, Shuryak I, Einstein AJ (2011) Impact of reduced patient life expectancy on potential cancer risks from radiologic imaging. *Radiology* 261(1):193–198
- Breslow NE, Day NE (1987) Statistical methods in cancer research. Volume II—The design and analysis of cohort studies. IARC Sci Publ 82:1–406
- Cardis E, Hatch M (2011) The Chernobyl accident—an epidemiological perspective. *Clin Oncol* 23(4):251–260
- Cardis E, Howe G, Ron E, Bebesko V, Bogdanova T, Bouville A, Carr Z, Chumak V, Davis S, Demidchik Y, Drozdovitch V, Gentner N, Gudzenko N, Hatch M, Ivanov V, Jacob P, Kapitonova E, Kenigsberg Y, Kesminiene A, Kopecky KJ, Kryuchkov V, Loos A, Pinchera A, Reiners C, Repacholi M, Shibata Y, Shore RE, Thomas G, Tirmarche M, Yamashita S, Zvonova I (2006) Cancer consequences of the Chernobyl accident: 20 years on. *J Radiol Prot* 26(2):127–140
- Chodick G, Ronckers CM, Shalev V, Ron E (2007) Excess lifetime cancer mortality risk attributable to radiation exposure from computed tomography examinations in children. *Isr Med Assoc J* 9(8):584–587
- Etard C, Sinno Tellier S, Aubert B (2010) [Exposure of the French population to ionizing radiation from medical diagnostic examinations in 2007] Institut de Radioprotection et de Sûreté Nucléaire (IRSN), Institut de Veille Sanitaire (InVS). http://www.irsn.fr/FR/Documents/RA2010/IRSN_INV_S_Rapport_Expri_032010.pdf. Accessed Jan, 31 2013
- Etard C, Sinno Tellier S, Empereur-Bissonnet P, Aubert B (2012) French population exposure to ionizing radiation from diagnostic medical procedures in 2007. *Health Phys* 102(6):670–679
- Furukawa K, Preston DL, Lonn S, Funamoto S, Yonehara S, Matsuo T, Egawa H, Tokuoka S, Ozasa K, Kasagi F, Kodama K, Mabuchi K (2010) Radiation and smoking effects on lung cancer incidence among atomic bomb survivors. *Radiat Res* 174(1):72–82
- Furukawa K, Preston D, Funamoto S, Yonehara S, Ito M, Tokuoka S, Sugiyama H, Soda M, Ozasa K, Mabuchi K (2013) Long-term trend of thyroid cancer risk among Japanese atomic-bomb survivors: 60 years after exposure. *Int J Cancer* 132(5):1222–1226
- Gelman A, Carlin JB, Stern HS, Rubin DB (2004) Bayesian data analysis (second ed). CRC/Chapman & Hall, Boca Raton
- Hammer GP, Seidenbusch MC, Schneider K, Regulla DF, Zeeb H, Spix C, Blettner M (2009) A cohort study of childhood cancer incidence after postnatal diagnostic X-ray exposure. *Radiat Res* 171(4):504–512
- Howe GR, McLaughlin J (1996) Breast cancer mortality between 1950 and 1987 after exposure to fractionated moderate-dose-rate ionizing radiation in the Canadian fluoroscopy cohort study and a comparison with breast cancer mortality in the atomic bomb survivors study. *Radiat Res* 145(6):694–707
- Hsu WL, Preston DL, Soda M, Sugiyama H, Funamoto S, Kodama K, Kimura A, Kamada N, Dohy H, Tomonaga M, Iwanaga M, Miyazaki Y, Cullings HM, Suyama A, Ozasa K, Shore RE, Mabuchi K (2013) The incidence of leukemia, lymphoma and multiple myeloma among atomic bomb survivors: 1950–2001. *Radiat Res* 179(3):361–382
- Huda W, Vance A (2007) Patient radiation doses from adult and pediatric CT. *Am J Roentgenol* 188(2):540–546
- IARC (2012) International agency for research on cancer (IARC). IARC monographs volume 100D—a review of human carcinogens: Radiation. Lyon, France

- ICRP (2005) Low-dose extrapolation of radiation-related cancer risk. ICRP Publication 99. Ann ICRP 35(4)
- Karlsson P, Holmberg E, Lundell M, Mattsson A, Holm LE, Wallgren A (1998) Intracranial tumors after exposure to ionizing radiation during infancy: a pooled analysis of two Swedish cohorts of 28,008 infants with skin hemangioma. *Radiat Res* 150(3): 357–364
- Kellerer AM, Nekolla EA, Walsh L (2001) On the conversion of solid cancer excess relative risk into lifetime attributable risk. *Radiat Environ Biophys* 40(4):249–257
- Kocher DC, Apostoaiei JA, Henshaw RW, Hoffman FO, Schubauer-Berigan MK, Stancescu DO, Thomas BA, Trabalka JR, Gilbert ES, Land CE (2008) Interactive radio epidemiological program (IREP): a web-based tool for estimating probability of causation/assigned share of radiogenic cancers. *Health Phys* 95(1):119–147
- Krille L, Jahnen A, Mildenerger P, Schneider K, Weisser G, Zeeb H, Blettner M (2011) Computed tomography in children: multicenter cohort study design for the evaluation of cancer risk. *Eur J Epidemiol* 26(3):249–250
- Krille L, Zeeb H, Jahnen A, Mildenerger P, Seidenbusch M, Schneider K, Weisser G, Hammer G, Scholz P, Blettner M (2012) Computed tomographies and cancer risk in children: a literature overview of CT practices, risk estimations and an epidemiologic cohort study proposal. *Radiat Environ Biophys* 51(2):103–111
- Land CE, Tokunaga M, Koyama K, Soda M, Preston DL, Nishimori I, Tokuoka S (2003) Incidence of female breast cancer among atomic bomb survivors, Hiroshima and Nagasaki, 1950–1990. *Radiat Res* 160(6):707–717
- Lechel U, Becker C, Langenfeld-Jager G, Brix G (2009) Dose reduction by automatic exposure control in multi detector computed tomography: comparison between measurement and calculation. *Eur Radiol* 19(4):1027–1034
- Linnet MS, Kim KP, Rajaraman P (2009) Children's exposure to diagnostic medical radiation and cancer risk: epidemiologic and dosimetric considerations. *Pediatr Radiol* 39(Suppl 1):S4–26
- Little MP (2001) Comparison of the risks of cancer incidence and mortality following radiation therapy for benign and malignant disease with the cancer risks observed in the Japanese A-bomb survivors. *Int J Radiat Biol* 77(4):431–464
- Little MP (2008) Leukaemia following childhood radiation exposure in the Japanese atomic bomb survivors and in medically exposed groups. *Radiat Prot Dosimetry* 132(2):156–165
- Lunn DJ, Thomas A, Best N, Spiegelhalter D (2000) WinBUGS: a Bayesian modelling framework: concepts, structure, and extensibility. *Stat Comput* 10:325–337
- Mathews JD, Forsythe AV, Brady Z, Butler MW, Goergen SK, Byrnes GB, Giles GG, Wallace AB, Anderson PR, Guiver TA, McGale P, Cain TM, Dowty JG, Bickerstaffe AC, Darby SC (2013) Cancer risk in 680,000 people exposed to computed tomography scans in childhood or adolescence: data linkage study of 11 million Australians. *Br Med J* 346:f2360
- Mattsson A, Ruden BI, Hall P, Wilking N, Rutqvist LE (1993) Radiation-induced breast cancer: long-term follow-up of radiation therapy for benign breast disease. *J Natl Cancer Inst* 85(20):1679–1685
- McLean D, Malitz N, Lewis S (2003) Survey of effective dose levels from typical paediatric CT protocols. *Australas Radiol* 47(2):135–142
- Mettler FA Jr, Huda W, Yoshizumi TT, Mahesh M (2008a) Effective doses in radiology and diagnostic nuclear medicine: a catalog. *Radiology* 248(1):254–263
- Mettler FA, Thomadsen BR, Bhargavan M, Gilley DB, Gray JE, Lipoti JA, McCrohan J, Yoshizumi TT, Mahesh M (2008b) Medical radiation exposure in the U.S. in preliminary results. *Health Phys* 95(5):502–507
- NCRP (2012) National council on radiation protection and measurements (NCRP) uncertainties in the estimation of radiation risks and probability of disease causation report No 171. NCRP Bethesda, MD
- Neglia JP, Robison LL, Stovall M, Liu Y, Packer RJ, Hammond S, Yasui Y, Kasper CE, Mertens AC, Donaldson SS, Meadows AT, Inskip PD (2006) New primary neoplasms of the central nervous system in survivors of childhood cancer: a report from the childhood cancer survivor study. *J Natl Cancer Inst* 98(21): 1528–1537
- NIH (2003) Report of the NCI-CDC working group to revise the 1985 NIH radioepidemiological tables. National Institutes of Health (NIH) Publication No. 03-5387. Bethesda, MD
- NRC (2006) Committee to assess health risks from exposure to low levels of ionizing radiation, national research council (NRC). Health risks from exposure to low levels of ionizing radiation: BEIR VII—Phase 2. National Academy of Sciences, Washington, DC
- Ozasa K, Shimizu Y, Suyama A, Kasagi F, Soda M, Grant EJ, Sakata R, Sugiyama H, Kodama K (2012) Studies of the mortality of atomic bomb survivors, Report 14, 1950–2003: an overview of cancer and noncancer diseases. *Radiat Res* 177(3):229–243
- Pearce MS, Salotti JA, Little MP, McHugh K, Lee C, Kim KP, Howe NL, Ronckers CM, Rajaraman P, Sir Craft AW, Parker L, Berrington de Gonzalez A (2012) Radiation exposure from CT scans in childhood and subsequent risk of leukaemia and brain tumours: a retrospective cohort study. *Lancet* 380(9840):499–505
- Pettorini BL, Park YS, Caldarelli M, Massimi L, Tamburrini G, Di Rocco C (2008) Radiation-induced brain tumours after central nervous system irradiation in childhood: a review. *Childs Nerv Syst* 24(7):793–805
- Phillips CV (2003) Quantifying and reporting uncertainty from systematic errors. *Epidemiology* 14(4):459–466
- Preston D, Lubin J, Pierce DA, McConney M (1993) *Epicure users guide*. Hirosoft, Seattle
- Preston DL, Mattsson A, Holmberg E, Shore R, Hildreth NG, Boice JD Jr (2002) Radiation effects on breast cancer risk: a pooled analysis of eight cohorts. *Radiat Res* 158(2):220–235
- Preston DL, Pierce DA, Shimizu Y, Cullings HM, Fujita S, Funamoto S, Kodama K (2004) Effect of recent changes in atomic bomb survivor dosimetry on cancer mortality risk estimates. *Radiat Res* 162(4):377–389
- Preston DL, Ron E, Tokuoka S, Funamoto S, Nishi N, Soda M, Mabuchi K, Kodama K (2007) Solid cancer incidence in atomic bomb survivors: 1958–1998. *Radiat Res* 168(1):1–64
- Richardson D, Sugiyama H, Nishi N, Sakata R, Shimizu Y, Grant EJ, Soda M, Hsu WL, Suyama A, Kodama K, Kasagi F (2009) Ionizing radiation and leukemia mortality among Japanese atomic bomb survivors, 1950–2000. *Radiat Res* 172(3):368–382
- Ron E (2003) Cancer risks from medical radiation. *Health Phys* 85(1):47–59
- Ron E, Lubin JH, Shore RE, Mabuchi K, Modan B, Pottern LM, Schneider AB, Tucker MA, Boice JD Jr (1995) Thyroid cancer after exposure to external radiation: a pooled analysis of seven studies. *Radiat Res* 141(3):259–277
- Ronckers CM, Doody MM, Lonstein JE, Stovall M, Land CE (2008) Multiple diagnostic X-rays for spine deformities and risk of breast cancer. *Cancer Epidemiol Biomarkers Prev* 17(3): 605–613
- Sadetzki S, Chetrit A, Freedman L, Stovall M, Modan B, Novikov I (2005) Long-term follow-up for brain tumor development after childhood exposure to ionizing radiation for tinea capitis. *Radiat Res* 163(4):424–432
- Schulze-Rath R, Hammer GP, Blettner M (2008) Are pre- or postnatal diagnostic X-rays a risk factor for childhood cancer? A systematic review. *Radiat Environ Biophys* 47(3):301–312

- Shore RE, Moseson M, Harley N, Pasternack BS (2003) Tumors and other diseases following childhood x-ray treatment for ringworm of the scalp (*Tinea capitis*). *Health Phys* 85(4):404–408
- Shrimpton PC, Jones DG, Hillier MC (1991) Survey of CT practice in the UK; Part 2: dosimetric aspects. London, UK
- Shrimpton PC, Hillier MC, Lewis MA, Dunn M (2006) National survey of doses from CT in the UK: 2003. *Br J Radiol* 79(948):968–980
- Sigurdson AJ, Ronckers CM, Mertens AC, Stovall M, Smith SA, Liu Y, Berkow RL, Hammond S, Neglia JP, Meadows AT, Sklar CA, Robison LL, Inskip PD (2005) Primary thyroid cancer after a first tumour in childhood (the Childhood Cancer Survivor Study): a nested case-control study. *Lancet* 365(9476):2014–2023
- Smith-Bindman R, Lipson J, Marcus R, Kim KP, Mahesh M, Gould R, Berrington de Gonzalez A, Miglioretti DL (2009) Radiation dose associated with common computed tomography examinations and the associated lifetime attributable risk of cancer. *Arch Intern Med* 169(22):2078–2086
- Smith-Bindman R, Miglioretti DL, Johnson E, Lee C, Feigelson HS, Flynn M, Greenlee RT, Kruger RL, Hornbrook MC, Roblin D, Solberg LI, Vanneman N, Weinmann S, Williams AE (2012) Use of diagnostic imaging studies and associated radiation exposure for patients enrolled in large integrated health care systems, 1996–2010. *JAMA* 307(22):2400–2409
- Stamm G, Nagel HD (2002) CT-expo—a novel program for dose evaluation in CT. *Rofo* 174(12):1570–1576
- Thierry-Chef I, Dabin J, Friberg EG, Hermen J, Istad TS, Jahnen A, Krille L, Lee C, Maccia C, Nordenskjold A, Olerud HM, Rani K, Rehel JL, Simon SL, Struelens L, Kesminiene A (2013) Assessing organ doses from paediatric CT scans—a novel approach for an epidemiology study (the EPI-CT study). *Int J Environ Res Public Health* 10(2):717–728
- Tukenova M, Guibout C, Hawkins M, Quiniou E, Mousannif A, Pacquement H, Winter D, Bridier A, Lefkopoulos D, Oberlin O, Diallo I, de Vathaire F (2011) Radiation therapy and late mortality from second sarcoma, carcinoma, and hematological malignancies after a solid cancer in childhood. *Int J Radiat Oncol Biol Phys* 80(2):339–346
- UNSCEAR (2006) Report of the United Nations scientific committee on the effects of atomic radiation. UNSCEAR 2006 report. Volume I. Annex A: epidemiological studies of radiation and cancer United Nations, New York
- UNSCEAR (2008) Report of the United Nations Scientific committee on the effects of atomic radiation. UNSCEAR 2008 report. Volume I. Annex A: medical radiation exposures. United Nations, New York
- Vaeth M, Pierce DA (1990) Calculating excess lifetime risk in relative risk models. *Environ Health Perspect* 87:83–94
- Wakeford R (2013) The risk of childhood leukaemia following exposure to ionising radiation—a review. *J Radiol Prot* 33(1):1–25